LAWRENCE
LIVERMORE
NATIONAL
LABORATORY

LLNL-BOOK-816634

Chapter 3 The Use of Surfactants in Enhanced Particle Removal During Cleaning

M. L. Free, Y. Zhu

November 10, 2020

Surfactants in Precision Cleaning

Disclaimer

Chapter 3

The Use of Surfactants in Enhanced Particle Removal During Cleaning

Michael L. Free[1] and Yakun Zhu[1,2]
[1]*Department of Materials Science & Engineering, University of Utah, Salt Lake City, UT, United States,* [2]*Materials Science Division, Lawrence Livermore National Laboratory, Livermore, CA, United States*

Chapter Outline

1 Introduction

1.1 Industrial Perspective

Many of the items we use daily must be manufactured in environments that require particulate materials, yet the particles that are essential to production must be removed to extremely low levels following the relevant manufacturing processes. A single particle remaining at a critical place on a semiconductor circuit during the manufacturing process can cause circuit failure in a finished integrated circuit. Consequently, particle removal techniques are

Surfactants in Precision Cleaning. DOI: https://doi.org/10.1016/B978-0-12-822216-4.00004-5

vital to electronic circuit manufacturing [1–20]. Other industries such as optical component manufacturing also rely upon particle removal techniques to create quality components with appropriate finishes.

In many industries, particles are handled in aqueous media, and particle removal from surfaces is also performed in aqueous media. Removal techniques vary from simple brush scrubbing techniques [21–24] and megasonic vibration [25–28] for wet surfaces to laser treatment [29,30] and water ice [31], CO_2 snow [32–34], and air [35] cleaning for dry surfaces.

Particles adhere to surfaces due to natural attractive forces between particles and surfaces. Surfactants can effectively reduce natural attractive forces between particles and surfaces, thereby enhancing particle removal. This chapter discusses the use of surfactants in enhancing particle removal from surfaces in aqueous environments, although the discussion presented here can also be applied to other environments [36]. Related information is also found elsewhere [37].

1.2 Historical Perspective

Powders have been used for grinding and polishing of jewelry and ornaments for millennia, yet an understanding of how particles interact with surfaces was relatively obscure until the 1940s [38]. Most of the present knowledge about particle–surface interactions can be related to research that developed in the 1940s. However, direct, accurate measurement of such interaction forces between fine particles and surfaces has only been possible with the inventions of the surface forces apparatus (SFA) and the atomic force microscope (AFM) that were developed in the 1970s and 1980s, respectively.

2 Surfactant Behavior in Solution

Surfactants are chemical compounds that are surface active or more prevalent at surfaces or interfaces than in bulk media due to their dual property nature. Molecules that are surface active in aqueous media consist of both hydrophobic and hydrophilic entities. The hydrophilic entity is polar in nature and gives the molecule its ability to dissolve in water. Most often the hydrophilic portion consists of an ionic functional group such as sulfate, sulfonate, carboxylate, or amine, or it contains hydrophilic segments such as ethylene oxide. The hydrophobic portion of the molecule consists typically of CH_2 groups that are usually connected in continuous alkyl chains consisting of 4–18 CH_2 groups and an end group of CH_3. Some surfactants contain a main alkyl chain section and up to three small branches of a smaller number of CH_2 groups and a CH_3 end group. An example of the structure of a surfactant is shown in Fig. 3.1 for cetyl benzyl trimethyl ammonium chloride. The hydrophobic portion of the molecule is nonpolar in nature and is

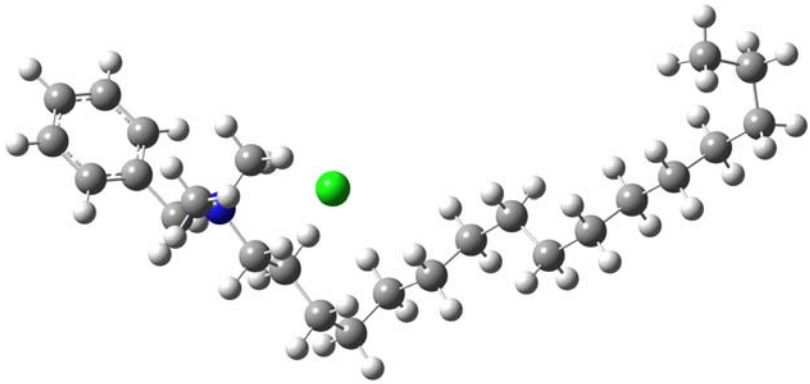

FIGURE 3.1 Molecular structure of benzyl cetyl trimethyl ammonium chloride for the lowest energy configuration with carbon, hydrogen, atoms nitrogen, as well as a chloride ion represented by gray, white, blue, and green spheres, respectively.

more favorably associated with other nonpolar entities, such as air or other hydrocarbon entities, rather than water. Consequently, the dual nature of surfactant molecules is more readily accommodated at water−air or water−oil interfaces than in bulk water. Moreover, surfactant molecules are found in higher concentrations at interfaces than in bulk aqueous media because the hydrophilic portion of the molecule can associate with water molecules at the same time as the hydrophobic portion associates with nonpolar media or hydrocarbon segments from other surfactant molecules. The tendency for surfactant molecules to associate with interfaces and other surfactant molecules leads to a high tendency for adsorption and aggregation, which increases as the hydrocarbon chain length increases and/or when the polarity of the solvent increases.

As surfactant concentration increases, the tendency of the surfactant to adsorb and/or form aggregate structures increases. At low concentrations, surfactant molecules do not have sufficient energy to form aggregates or adsorb at high concentrations at interfaces as illustrated in Fig. 3.2, although they adsorb at higher concentrations at interfaces than in bulk media. At moderate concentration levels, surfactant molecules also adsorb at interfaces at higher levels than in the bulk solution.

The accumulation of surfactant molecules at interfaces such as the air−water interface results in lowering of the surface tension. In other words, the accumulation of surfactant molecules at interfaces lowers the interfacial energy due to the fact that the surfactant molecules have both hydrophilic and hydrophobic sections that are attracted to the water (polar) and air (nonpolar) phases, respectively.

Surface tension is often measured using a balance and a suspended hydrophilic object such as a plate or a ring. As shown in Fig. 3.3, the presence of

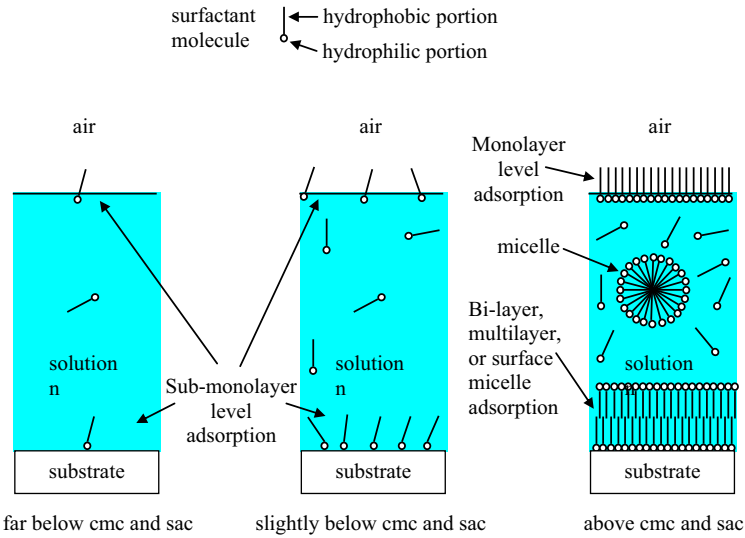

FIGURE 3.2 Schematic diagrams illustrating surfactant aggregation and adsorption as a function of relative surfactant concentration.

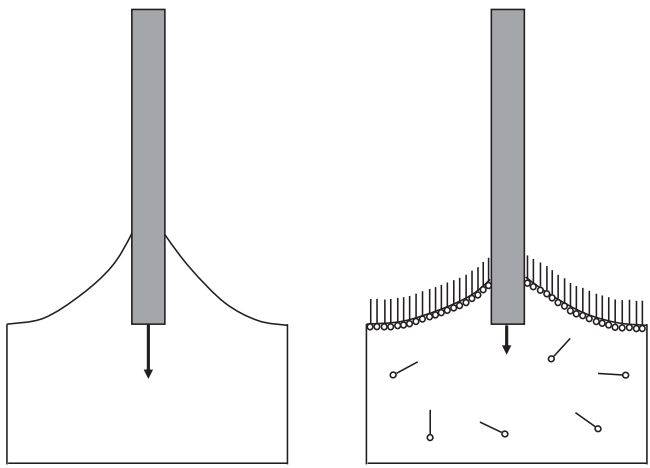

FIGURE 3.3 Schematic comparison of surface tension force exerted by water on a plate with (right side) and without surfactant (left side) present.

surfactant molecules at the air−water interface lowers the tendency of the water to climb up a hydrophilic substrate such as the plate shown in the figure, resulting in a reduced downward force on the object as indicated by the arrows in Fig. 3.3. A typical plot of surface tension versus the natural

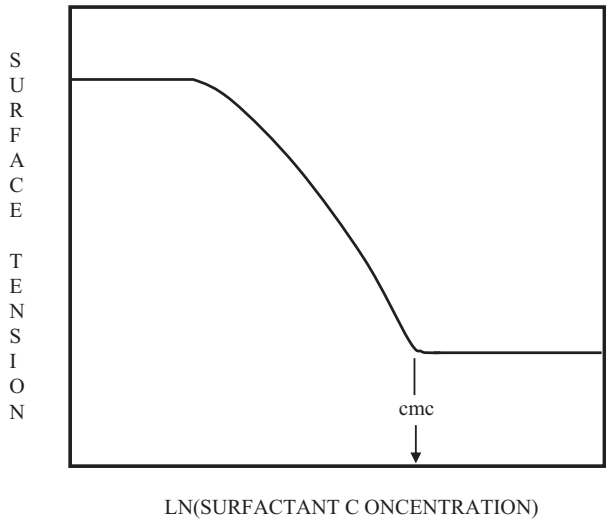

FIGURE 3.4 Sketch of typical surface tension versus ln(surfactant concentration) plot showing the critical micelle concentration (cmc).

logarithm of the concentration is shown in Fig. 3.4. Note that the surface tension decreases rapidly with increasing surfactant concentration above a minimum concentration level. At higher concentrations, it reaches a minimum value at a specific concentration level that is known as the critical micelle concentration (cmc) that will be discussed in more detail later.

The excess concentration of surfactant at an interface can be quantified using surface tension data and the Gibbs equation. The surface excess or concentration at the interface that is in excess of the bulk concentration Γ below the cmc for constant temperature tests in which no phase transformations occur can be expressed as [39]:

$$\Gamma = -\frac{1}{RT}\left(\frac{\mathrm{d}\gamma}{\mathrm{dln}(c)}\right) \tag{3.1}$$

where R is the gas constant, T is the absolute temperature, γ is the surface tension, and c is the concentration of surfactant. Note that the slope of the surface tension plot shown in Fig. 3.4 is used in the calculation of the surface excess, which is also nearly equivalent to the adsorption density.

The adsorption of surfactant molecules at interfaces is often evaluated using the Langmuir model, which begins with the equilibrium adsorption reaction:

$$\mathrm{A} + \mathrm{S} = \mathrm{AS} \tag{3.2}$$

where A is the adsorbate, S is the surface site available for adsorption, and AS represents a surface site on which the adsorbate, A, is adsorbed. Using a simple equilibrium expression, the equilibrium constant K'_A can be expressed as:

$$K'_A = \frac{C_{AS}}{C_A C_S} \tag{3.3}$$

where C_{AS} is the surface concentration of adsorbed adsorbate, C_S is the surface concentration of unoccupied surface adsorption sites, and C_A is the bulk solution concentration of adsorbate. Using Eq. (3.3) with a surface site balance and substitution for the concentration of available sites ($C_S = C_{tot} - C_{AS}$) leads to a common expression for the fraction of surface θ covered by the adsorbate:

$$\theta = \frac{C_{AS}}{C_{tot}} = \frac{K'_A C_A}{1 + K'_A C_A} \tag{3.4}$$

where C_{tot} is the total number of available sites for adsorption, including occupied and unoccupied. However, it should be noted that this expression is only valid at concentration levels below those needed for surfactant aggregation. It is also important to realize that surfactant aggregation at solid surfaces, which is referred to as the surface aggregation concentration (sac), often occurs at concentrations that are below the cmc. Thus, the cmc applies to surfactant micelle aggregate formation in solution and the sac applies to surfactant aggregate formation on solid surfaces.

As the surfactant concentration reaches levels that exceed the sac, the surfactant molecules have already exhausted interfacial adsorption sites at the monolayer level, and the free energy of the system warrants additional association and aggregation in the form of spherical or cylindrical micelles as well as bilayers and/or multilayers at interfaces. Similarly, above the cmc micelles form in solution. Micelles are spherical or cylindrical aggregates of surfactant molecules in which the hydrocarbon portions of the molecules associate with the hydrocarbon portions of other surfactant molecules in the interior of the structure. The outer wall of the micelle structure is formed with the hydrophilic functional groups of the surfactant molecules as depicted in Fig. 3.2. Fig. 3.2 illustrates the concentration dependence of surfactant adsorption relative to surfaces.

The tendency for surfactant molecules to aggregate and associate at interfaces is influenced strongly by the length of the hydrocarbon portion of the surfactant molecules. As the hydrocarbon chain portion of the surfactant molecule increases in length, the tendency of the surfactant to aggregate or adsorb increases to relieve energetically unfavorable interactions between polar solvent molecules and nonpolar hydrocarbon groups. Consequently, the critical concentration for aggregation (cmc or sac) decreases as the chain length increases because the aggregation event occurs at decreasing concentration levels as the hydrocarbon chain length increases. The effect of

TABLE 3.1 Comparison of Hydrocarbon Chain Length and Critical Micelle Concentration (cmc) for Alkyl Trimethyl Ammonium Chlorides in Water [36].

Number of Alkyl CH_2 Segments	cmc (M)
10	6.3×10^{-2}
12	1.9×10^{-2}
14	4.5×10^{-3}
16	1.3×10^{-3}
18	3.4×10^{-4}

increasing hydrocarbon chain length on the aggregation concentration (cmc for solutions) can be observed readily from the data in Table 3.1. The data in Table 3.1 indicate that the cmc of alkyl trimethyl ammonium chloride surfactants decreases by approximately a factor of three for every two CH_2 units added to the surfactant molecule.

The tendency for surfactant molecules to adsorb and/or aggregate in solution is also influenced by the solution environment. As the solution becomes more polar, the tendency for surfactant molecules to aggregate in solution and/or adsorb at interfaces increases. One factor that quantifies the polar nature of the solvent is the ionic strength. Consequently, the effect of ionic strength on surfactant aggregation is very significant as evidenced by the cmc values given in Table 3.2. Note that the cmc values in Table 3.2 are considerably lower in high ionic strength media. The data in Table 3.2 also indicate that the effect of ionic strength is more pronounced as the hydrocarbon chain length increases, indicating that the surfactant molecules with longer alkyl hydrocarbon chains have an increased tendency to leave the solution to form surface and solution aggregates as the solvent polarity increases.

The combined effects of environment and hydrocarbon chain length on the cmc of a surfactant can be predicted based on a combination of theory and empirical information. The following equation is very useful in predicting the cmc (or sac if slightly different values for x, $\Delta G_{c.l.}$, and k are used) of surfactant molecules under a variety of chain length and ionic strength scenarios [40]:

$$\text{cmc} \cong \exp\left(\frac{1}{RT}\left[(L-x)\Delta G_{c.l.} + k(L-x)RT\ln(\gamma_m)\right]\right) \tag{3.5}$$

where R is the gas constant, T is the absolute temperature, L is the total number of consecutive CH_2 units in the surfactant molecule, $\Delta G_{c.l.}$ is the free energy increment for each CH_2 unit (-1500 J/mol is a good estimate for some

TABLE 3.2 Comparison of Surfactant Critical Micelle Concentration (cmc) Values as a Function of Ionic Strength and Surfactant Type [36,38].

Surfactant	Ionic Strength	Chain Length (No. of CH_2 Groups)	cmc (M)
Sodium octyl sulfate	0.3	8	6.7×10^{-2}
Sodium octyl sulfate	0.07	8	1.3×10^{-1}
Sodium decyl sulfate	0.3	10	6.9×10^{-3}
Sodium decyl sulfate	0.007	10	3.3×10^{-2}
Sodium dodecyl sulfate	0.3	12	7×10^{-4}
Sodium dodecyl sulfate	0.0007	12	8.1×10^{-3}
Cetylpyridinium chloride	1.0	16	3×10^{-6}
Cetylpyridinium chloride	0.0003	16	3×10^{-4}

surfactants [40–42]), x is the number of CH_2 units in the surfactant molecule necessary to initiate surface activity (usually around 5), k is a solvent polarity factor (usually 1.0–1.5 for surfactants for which L is 12–18 [40–43]), and γ_m is the activity coefficient determined using an ionic activity coefficient equation, such as the Davies equation, which can be expressed as [44]:

$$\gamma_m = 10^{-0.5083z^2}\left(\frac{\sqrt{I}}{1+\sqrt{I}} - 0.2I\right) \tag{3.6}$$

at 25°C, where z is the charge of the surfactant ion (usually 1) and I is the ionic strength given by [44]:

$$I = 0.5\sum_{j=1}^{n} m_j z_j^2 \tag{3.7}$$

where $j = 1$ to n represents all positively and negatively charged species in solution and m is the molality. If the aqueous solution is highly concentrated (> 1 M) in the counterion of surfactant molecule, for example, Cl^- or salts, Pizter's method is recommended for the calculation of the activity coefficient [41,45,46].

More exact values of the various constants can be obtained using cmc data based on calibration plots as described by Free and coworkers [40]. The work of Free and coworkers [40] was further extended to calculate the cmc of mixed surfactants in aqueous phase from the expression given next [41–43]:

$$\Gamma^w = \frac{1}{\sum_i x_i\left(\gamma_c C_c\right)^{\delta_i}\left(1/\Gamma_i^p\right)^{(1+\delta_i)}} \tag{3.8}$$

where x_i is the bulk mixed molar fraction of surfactant I; Γ_i^p is the aqueous cmc of surfactant i in pure water (i represents surfactant 1, 2, or 3, . . .); δ_i is counterion-binding coefficient with respect to surfactant i based on best fit of experimental data. δ_i is nearly constant for a series of homologous surfactants and is also constant as a function of salt concentration (low to medium depending on specific surfactant class: 0−1). Note that the counterion-binding coefficient δ_j in the advanced cmc model is with respect to counterion j and different from δ_i. C_c is the concentration of ion dissociated from electrolyte and from ionic surfactant in aqueous solution. γ_c is the mean activity coefficient of ions in aqueous solution. Comparisons between experimental and predicted cmc for different surfactant mixtures are given in Fig. 3.5.

More advanced thermodynamic models for cmc prediction considering related interactions between surfactant molecules, environmental parameters,

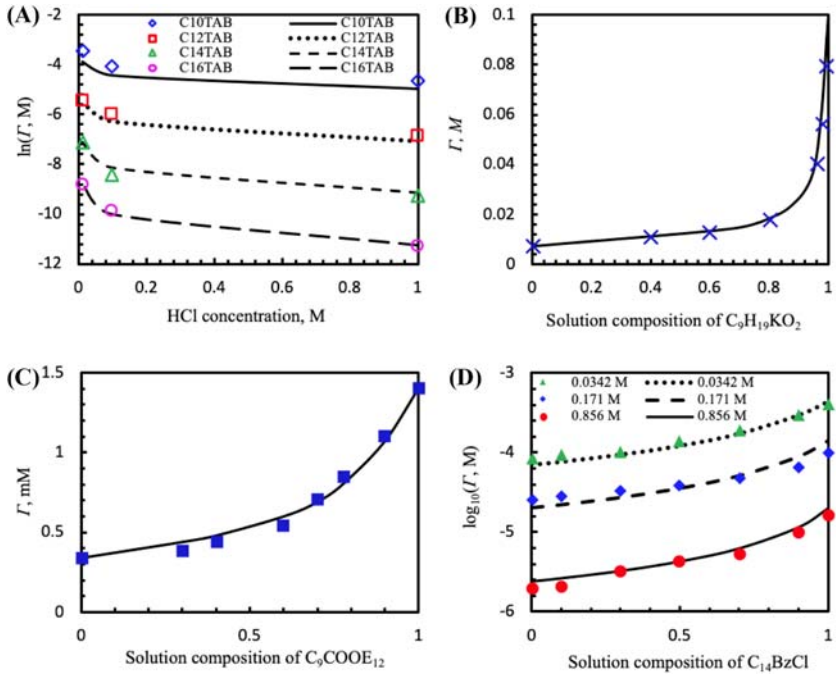

FIGURE 3.5 Comparison between predicted and experimental cmc (Γ): (A) cmc of pure C_nTAB as a function of HCl concentration in solution at $T = 25°C$; (B) cmc of binary mixed nonionic surfactants ($C_9H_{19}KO_2$ and $C_{11}H_{23}KO_2$) as a function of bulk mixed molar fraction of $C_9H_{19}KO_2$ at $T = 25°C$; (C) cmc of binary mixed nonionic surfactants (C_9COOE_{12} and $C_{11}COOE_{12}$) as a function of bulk mixed molar fraction of C_9COOE_{12} at $T = 25°C$ without salt; (D) cmc of ternary mixed homologous cationic surfactants BAC ($C_{12}BzCl$, $C_{14}BzCl$, and $C_{16}BzCl$) as a function of mixed molar fraction of $C_{14}BzCl$ with NaCl concentrations of 0.0342, 0.171, or 0.856 M at $T = 40°C$; $C_{12}BzCl$ and $C_{16}BzCl$ are equal-molar mixed.

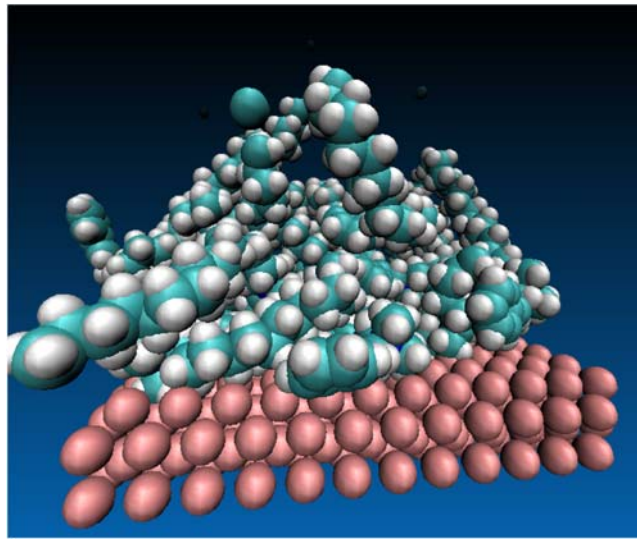

FIGURE 3.6 Molecular dynamics simulation of cetyl benzyl trimethyl ammonium chloride ion aggregation and adsorption at an iron surface. The red, white, green, and blue spheres represent iron, hydrogen, carbon, and nitrogen, respectively. Chloride ions and water molecules were present in the simulation but are not shown. *Image courtesy Dr. Keith Prisbrey.*

such as temperature, salt, and ionic strength effects, are available in our further extended cmc work [47–49] and in the literature [45,46,49–56], but they generally require more information for their applications.

One example of more advanced modeling for surfactant aggregation involves the use of molecular dynamics simulations. Molecular dynamics simulations utilize basic laws of physics and atomic level interaction forces to predict movements of molecules in a variety of environments. An example of a molecular dynamics simulation result for cetyl benzyl trimethyl ammonium chloride surfactant aggregation and adsorption on an iron surface is shown in Fig. 3.6. Related molecular dynamics simulation information is found in the literature [57–63].

Understanding how surfactants behave in solution in terms of their tendency to aggregate and adsorb at interfaces is a critical prerequisite to understanding how they can enhance particle removal as will be demonstrated in a subsequent section.

3 Interaction Forces and Particle Removal

3.1 Introduction to Interaction Forces

Interaction forces between molecules and surfaces can be very powerful and influential. The forces between molecules determine the physical state of

groups of molecules. Such groups of molecules make up surfaces and become the origin of the forces that exist between surfaces. The forces between molecules and surfaces in aqueous media are often separated into electrostatic, van der Waals, structural, and hydrophobic forces. In situations involving nonimmersion scenarios, capillary forces must also be considered, although in the remainder of this chapter they will be neglected.

Van der Waals forces arise from the interaction of atomic and/or molecular dipole interactions [46]. van der Waals forces between molecules or atoms are attractive in nature, and such attractive forces exist even when the atom or molecule does not have a permanent dipole, since the dipole can be induced [64]. The van der Waals force between a spherical particle and a plate can be expressed as [64]:

$$F(h) = -\frac{Ar}{6h^2} \tag{3.9}$$

where A is the Hamaker constant, r is the radius of curvature of the spherical particle, and h is the separation distance between the particle and the plate.

The electrostatic force between a spherical particle and a plate is given as [64]:

$$F(h) = \frac{128\pi R\rho_\infty kT\gamma_1\gamma_2}{\chi}\exp(-\chi h) \tag{3.10}$$

where the surface charge for each surface (1 and 2 as denoted by subscript) is defined as [64]:

$$\gamma_{(1\text{ or }2)} = \tanh\left(\frac{ze\Psi_{0(1\text{ or }2)}}{4kT}\right) \tag{3.11}$$

and the Debye length, χ, is given as [64]:

$$\chi = \left(\frac{2000e^2IN_A}{\varepsilon_0\varepsilon_m kT}\right)^{1/2} \tag{3.12}$$

where z is the ion valence, e is the electrical charge, ρ_∞ is the bulk dissolved ion density, $\Psi_{0\ (1\text{ or }2)}$ is the surface potential for the surface of interest (surface 1 or 2). I is the ionic strength ($0.5\Sigma z^2\rho_\infty$ for all positive and negative ions), N_A is Avogadro's number, k is the Boltzmann constant, ε_0 is the dielectric permittivity of vacuum, and ε_m is the dielectric constant of the medium between the two surfaces.

In many aqueous environments involving hydrophilic surfaces, the forces between surfaces are dominated by the electrostatic and van der Waals forces, since structural forces tend to be oscillatory in nature and tend to average to a near-zero net effect. In other words, the structural forces show up as oscillations above and below the other net forces. The trend of the other forces remains dominant despite the local oscillations that arise as

surfaces come close to contact and individual layers of water are removed or added in a stepwise manner, causing stepwise oscillations in the overall force. Such structural oscillations are often observed within a few nanometers of the surface [38].

The use of the combination of electrostatic and van der Waals forces to describe surface interactions was demonstrated extensively by Derjaguin, Landau, Verwey, and Overbeek [64]. Their work and use of surface force theory has become widely known as the DLVO theory [64]. Furthermore, when only the electrostatic and van der Waals forces are considered in a surface force analysis, the resulting interaction force is sometimes referred to as the DLVO force. In situations involving hydrophilic substrates in low ionic strength media, the DLVO theory is often adequate to describe the forces between particles and surfaces before contact occurs.

Although the DLVO theory accounts for surface forces in many situations, it does not describe the effect of forces between hydrophobic surfaces that can far exceed the attractive forces predicted by the DLVO theory. The strong, attractive forces between hydrophobic surfaces are often referred to as hydrophobic forces [63–67]. There is considerable debate regarding the origin of these forces [64]. However, the most commonly accepted hypotheses suggest that the forces are related to water structuring effects and/or gas entrainment/cavitation effects [64].

3.2 Measurement of Surface Forces

Surface forces can be measured by different instruments. Most commonly, surface forces are measured using the AFM and the SFA, both of which are capable of measuring interaction forces between surfaces at varying separation distances. The AFM, which was developed in the mid-1980s by Binnig and coworkers [68], utilizes a thin cantilever beam that bends in response to surface forces experienced by the tip as the surface is moved closer to it by a piezo crystal (Fig. 3.7). The change in the angle of the cantilever causes a change in the angle of the light that is reflected off the tip of the cantilever (Fig. 3.7). Because the light that is reflected off the cantilever is measured by a set of detectors with respect to both quantity and position, a determination of the force can then be made based on the cantilever properties and dimensions combined with the position and intensity of the deflected light. The distance is measured based on the applied piezo crystal voltage change combined with the properties of the piezo crystal actuator and a calibration procedure.

The SFA, which was developed prior to the AFM [38], has a significantly different design than the AFM (Fig. 3.8). The SFA consists of a cantilever to measure the force based on deflection as is done in the AFM. However, the separation between surfaces is measured using white light diffraction techniques that utilize a spectrometer to analyze the various wavelengths of light.

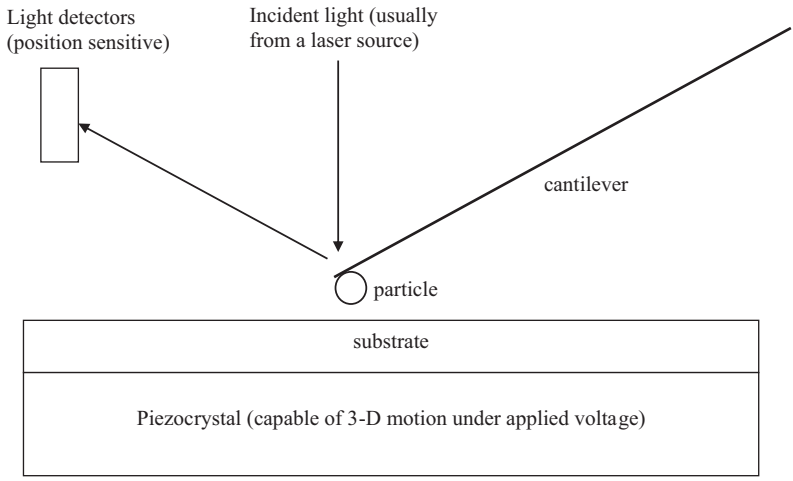

FIGURE 3.7 Schematic diagram of an atomic force microscope.

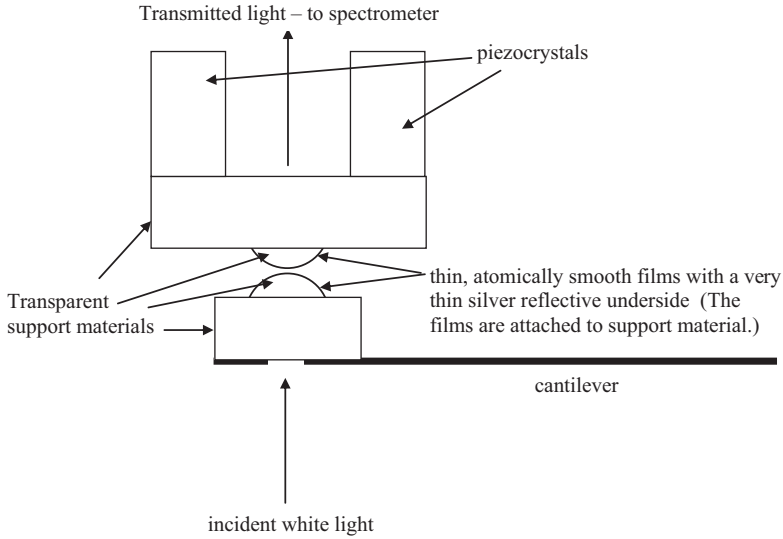

FIGURE 3.8 Schematic diagram of a surface forces apparatus.

The surfaces that are used in the SFA must be atomically smooth, and they are generally mounted as thin films onto cylindrical, optically transparent support structures as shown in Fig. 3.8. The films must be coated with a very thin layer of silver or other reflective metal on the back side to allow significant light transmission while also allowing significant reflected light. As light reflects between the silvered back sides of the layers that approach

contact, interference fringe patterns are created. The interference fringe patterns can be analyzed spectroscopically to determine the separation distance between surfaces to within approximately 1 Å [38].

3.3 Adhesion

Particles adhere to surfaces due to favorable interaction forces between them. The dominant force of attraction between particles and surfaces is the van der Waals force. This force is so strong that the particle and surface are deformed upon natural contact. The extent of the deformation is determined by the elastic moduli of the substances involved as well as the magnitude of the attractive force. The deformation is large for soft materials and small for hard ones. Several theories have been proposed to calculate the deformation and forces involved in the adhesion of particles to surfaces [69–74]. The attractive forces remain the same despite the material deformation, but the effect of material deformation leads to an increased requirement for particle removal [38].

Adhesion forces can be estimated from the sum of the known forces. The force calculation is usually made at a particle-to-surface separation distance that is between 0.1 and 0.5 nm in aqueous media. The separation distance is not zero because the continuum theories used to derive the force expressions do not accurately account for the discrete nature of the atoms at the interfaces at close separation distances. Also, in aqueous media, surface layers of water are bonded to the surfaces and may affect the effective separation distance. Another approach, the surface-free energy/acid–base theory [75], also provides useful approximations of adhesion forces, although this technique will not be discussed further because it cannot be applied as easily to systems involving surfactant adsorption as the sum-of-forces approach described previously. In addition, the surface-free energy/acid–base theory does not account for electrostatic forces that can be important in particle–surface systems.

3.4 Particle Removal Forces

Particles can be removed from surfaces by pulling, rolling, or sliding them off, yet each of these techniques requires an external force. The most common external force that is used for these techniques is fluid drag that is created by fluid flow. The force of fluid drag on a particle under laminar flow conditions can be expressed as [76]:

$$F = -3\pi d_0 V \mu \tag{3.13}$$

where F is the force, d_0 is the particle diameter, V is the fluid velocity, and μ is the viscosity.

However, the fluid velocity at any given position relative to the particle is proportional to distance above the substrate surface [77]. Consequently, the fluid elements that are capable of moving the particle are located at a distance from the surface that is proportional to the particle diameter. Thus, as is intuitively apparent, the force of removal due to fluid drag is surface area dependent, based on fluid flow near a substrate surface and an attached particle at the surface. Consequently, the actual removal force on a particle at a surface due to fluid drag is directly proportional to the diameter squared. Thus, as particles become smaller, the force available for removal from fluid movement decreases rapidly. In contrast the forces such as van der Waals and electrostatic forces that control adhesion are linearly related to particle diameter and do not diminish as rapidly as the traditional removal forces. Therefore, large particles are easily washed away from surfaces, while small particles are not unless the surface forces are reduced or the removal forces enhanced, although in this chapter only surface force modification using surfactants will be discussed as a means of enhancing particle removal.

3.5 Modification of Surface Forces Using Surfactants

The adsorption of surfactant molecules at the surfaces of particles and substrates can alter the van der Waals attractive force between the particles and substrates as well as the electrostatic, structural, and hydrophobic forces.

The effect of surfactant adsorption on the van der Waals force is most easily quantified using an approximate expression developed by Israelachvili [38] (for surfaces with adsorbed layers that are separated by a medium such as water) that has been modified from a plate−plate interaction force to a plate−sphere interaction force using the Derjaguin approximation [65]:

$$F(h) = \frac{R}{6}\left[\frac{A_{432}}{h^2} - \frac{\sqrt{A_{545}A_{323}}}{(h+t_p)^2} - \frac{\sqrt{A_{121}A_{343}}}{(h+t_s)^2} + \frac{\sqrt{A_{121}A_{545}}}{(h+t_p+t_s)^2}\right] \tag{3.14}$$

where 1 is the surface of the substrate, 2 is the coating on the substrate surface, 3 is the medium separating the surfaces, 4 is the coating on the particle, 5 is the surface of the particle, t_s is the thickness of the coating on the substrate surface, and t_p is the thickness of the coating on the particle surface. However, to utilize this force expression, it is necessary to know the Hamaker constants between the various substances. A useful expression for determining the Hamaker constant based on Lifshitz theory is given by Israelachvili as [38]:

$$A_{132} \approx \frac{3}{4}kT\left(\frac{\varepsilon_1-\varepsilon_3}{\varepsilon_1+\varepsilon_3}\right)\left(\frac{\varepsilon_2-\varepsilon_3}{\varepsilon_2+\varepsilon_3}\right) + \frac{3h\nu_e}{8\sqrt{2}}\left[\frac{(n_1^2-n_3^2)(n_2^2-n_3^2)}{(n_1^2+n_3^2)^{1/2}(n_2^2+n_3^2)^{1/2}[(n_1^2+n_3^2)^{1/2}+(n_2^2+n_3^2)^{1/2}]}\right] \tag{3.15}$$

where A_{132} is the nonretarded Hamaker constant between surfaces 1 and 2 across medium 3, k is the Boltzmann constant, T is the absolute temperature, ε is the dielectric constant of specified medium, h is Planck's constant, v_e is the average absorption frequency, and n is the refractive index.

The justification for using a multiple-layer model to determine the effect of surfactant adsorption on the van der Waals force is made on the basis of experimental observation, which shows that the effect of the adsorbed layer on the van der Waals force becomes increasingly important as the surfaces approach contact [38]. The adsorbed layer(s) of surfactant molecules also provides a steric barrier to direct contact between the particle and the substrate.

The adsorption of surfactant molecules on the substrate and particle surfaces also tends to significantly alter the charges on the surfaces as is depicted with an adsorbed cationic surfactant molecule at a charged surface in Fig. 3.9. The effect of surfactant adsorption depends on the existing charge prior to surfactant adsorption, the charge of the surfactant molecule, and the surface concentration of surfactant on each surface after adsorption. In some cases the adsorption of ionic surfactant can have a very substantial effect on the electrostatic force between the substrate and particles in solution. In some particle removal applications, the particles have a charge that is opposite to that of the substrate, making the natural electrostatic force between the surfaces an attractive one (negative force). If an ionic surfactant adsorbs on the surfaces of the particles and the substrate, which is generally observed, both types of surfaces will likely develop the same charge as the surfactant, making the electrostatic interaction force between the surfaces a positive or repulsive force, thereby reducing particle adhesion and enhancing particle removal. In cases involving substrates and particles with similar natural charge, the adsorption of properly selected ionic surfactant molecules can enhance the existing repulsive electrostatic force. Thus, in most cases

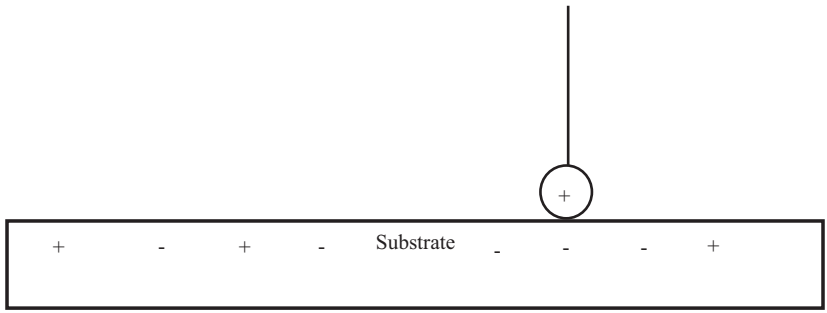

FIGURE 3.9 Schematic diagram of a cationic surfactant molecule adsorbed onto a charged substrate. Note that the charge on the substrate is generally due to adsorbed ions such as OH^- and H^+ that are not shown. Also note that water molecules, which play an important role at interfaces in aqueous media, are not shown.

the adsorption of ionic surfactant molecules facilitates particle removal by providing or enhancing electrostatic repulsive forces in addition to providing a steric barrier to direct contact between the particle and the substrate.

Although it is clear that surfactant adsorption can reduce van der Waals attractive forces and create or enhance electrostatic repulsion between particles and surfaces, surfactant adsorption can lead to a hydrophobic attractive force, which tends to make particle removal more difficult. Because particle removal is the objective of this chapter, it is desired that the adsorbed surfactant molecules be arranged with hydrophilic ends projecting into aqueous media or hydrophobic ends projecting into a hydrophobic solvent. Using the illustrations shown in Fig. 3.10, it is easily observed that for aqueous media and naturally hydrophilic surfaces, this desired outcome is achieved only above the sac where bilayers, multilayers, or surface micelles (spherical or cylindrical) form to provide an exposed interface of hydrophilic functional groups.

Surfactant adsorption and aggregation on naturally hydrophobic surfaces begins with the adsorption of surfactant in the opposite orientation to that shown in Fig. 3.10 with the hydrophobic tails attaching at the surface and the hydrophilic head groups extended into solution. Similarly, hemimicelles and hemicylindrical micelles adsorb on hydrophobic surfaces with the hydrophobic tails of the surfactant molecules attached to the surface. Hydrophobic surfaces in aqueous media can achieve some level of removal when

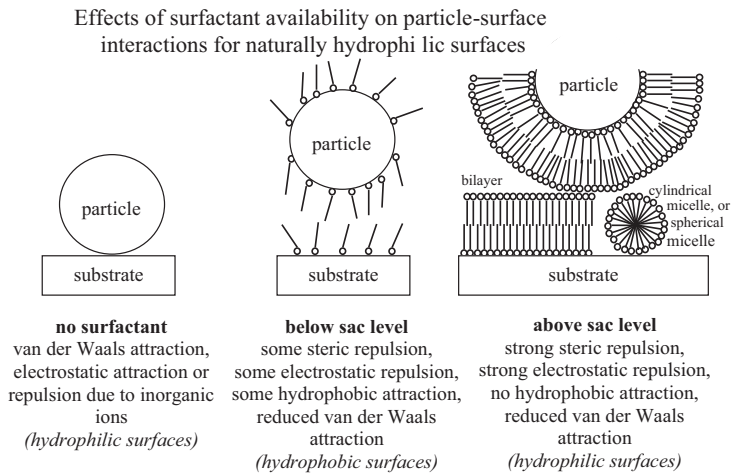

FIGURE 3.10 Schematic diagrams illustrating the effect of surfactant concentration and adsorption on the particle−substrate interaction for surfaces that are naturally hydrophilic. Note that water molecules and other ions such as counterions have been omitted to simplify the drawings. Although the diagram shows bilayer formation above the sac, it is also common to observe surface micelles and multilayer level adsorption above the sac.

sufficient surfactant is present due to the presence of hydrophilic, charged surfactant head groups that extend away from the surface, contributing to hydrophilicity and charging, while also mitigating hydrophobic attraction to other hydrophobic surfaces.

Fig. 3.11 shows an AFM image of cetyl trimethyl ammonium chloride surfactant adsorbed on a hydrophobic pyrolytic graphite surface in rows of hemicylindrical micelles. The corresponding width of each row of hemicylindrical micelles is approximately 5 nm, which corresponds approximately with the length of two surfactant molecules plus additional row separation due to electrostatic repulsion between functional groups.

The effect of the orientation of the head group and hydrocarbon tail of the adsorbed surfactant molecules on the attractive hydrophobic force has been demonstrated by Freitas and Sharma [78], who showed a strong attractive force between hydrophilic silica particles and substrates below the sac, where hydrocarbon tails of adsorbed surfactant molecules extended into solution to produce a hydrophobic interface. However, above the sac, where only functional groups from a bilayer, multilayers, or surface micelles extended

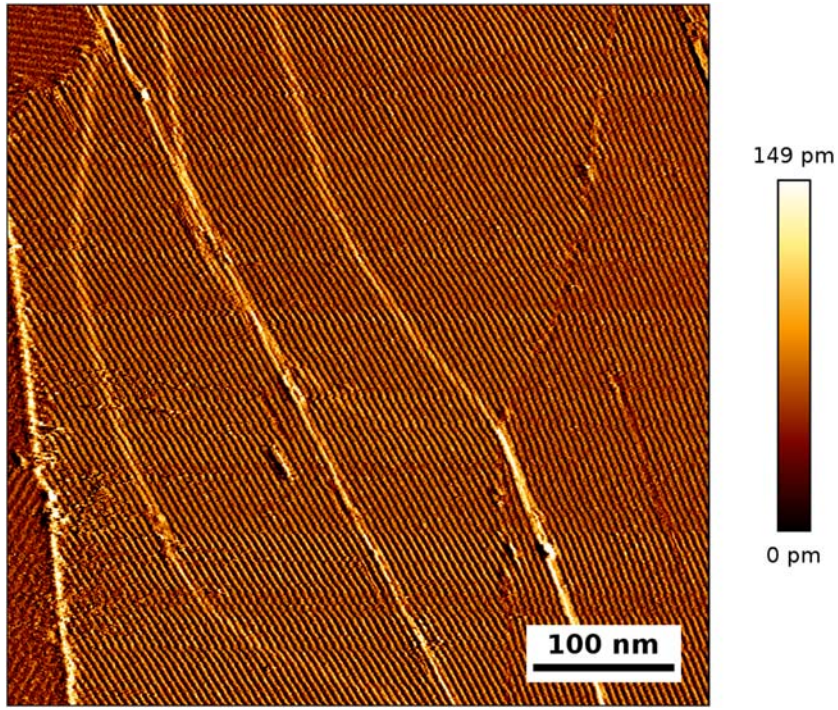

FIGURE 3.11 AFM (Model JPK NanoWizard 3a Ultra) image of cetyl trimethyl ammonium chloride surfactant adsorbed as hemicylindrical micelles on a highly oriented pyrolytic graphite surface.

into aqueous media, the interaction force became very weak. It should be noted that no complete explanation for such hydrophobic interaction forces has been developed.

The net force between a particle and a substrate can be calculated using the equations described previously for the van der Waals and electrostatic force components, which are the most important overall forces as long as the surfaces are hydrophilic. Many surface force studies have been performed [79–93], and there is at least general agreement that experimental data can be modeled using the applicable theory [83,93]. Thus, it is useful to examine the effects of surfactant adsorption on the net interaction force between a particle and a substrate. There is significant interest in understanding particle–substrate interaction forces in the context of removing particles from surfaces that is of particular interest in the electronics manufacturing industry, particularly in association with the process of chemical mechanical planarization and related cleaning of wafers [94–99].

A sample comparison of DLVO forces that have been normalized by dividing by particle radius versus the separation distance between bare and film-covered surfaces is presented in Fig. 3.12 for an ideal alumina sphere that is approaching a quartz surface in aqueous media at a near-neutral pH.

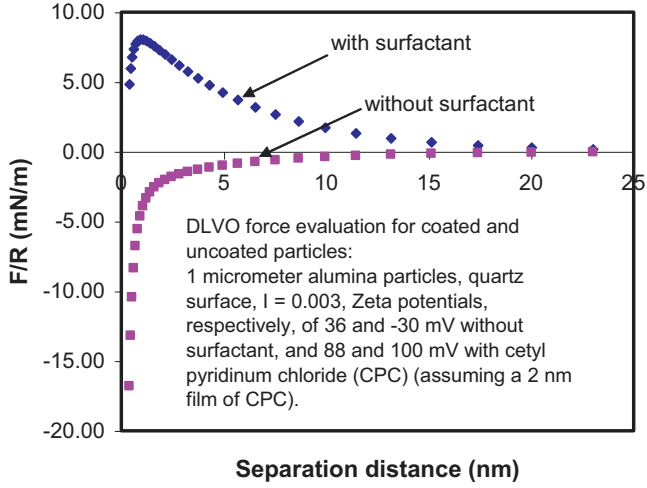

FIGURE 3.12 Comparison of normalized DLVO force (normalized by dividing by particle radius) versus separation distance for alumina particles approaching a quartz surface. Note that the Hamaker constant was calculated using Eq. (3.14) with refractive index and dielectric constant data from Ref. [64]. The forces were calculated using Eqs. (3.3), (3.9–3.11), and (3.13). Note that the zeta potential values shown in the figure are values that were measured using ground quartz and alumina particles in a 0.003 M KCl solution at 22°C with and without 0.0028 M cetylpyridinium chloride as indicated. The surface potential, ψ, was calculated based upon the zeta potentials using the relationship: ψ = zeta potential [exp(−χ/1 nm)] (assumes that the zeta potential is 1 nm from surface).

Note that the net normalized force is highly negative as the particle approaches the surface when no surfactant is present. The attraction in the absence of surfactant is due to the van der Waals attractive force and an attractive electrostatic force. However, in the presence of cetylpyridinium chloride (CPC) surfactant at a level of 0.0028 M, which is well above the cmc of 0.0003 M (also above the sac of around 0.0001 M) for this solution, it results in a positive or repulsive force at separation distances that are representative of contact. It should be noted that in applying the DLVO theory in aqueous media, contact is assumed to occur at a separation distance greater than zero (often around 0.4 nm) as explained previously. In this particular case the result of adding surfactant is quite dramatic because the surfaces had opposite charges prior to surfactant adsorption. Thus, the addition of the surfactant made an enormous difference in the surface forces. In systems involving similar surfaces, surfactant molecules do not alter the forces as dramatically, yet the addition of surfactant molecules can enhance repulsive forces as shown in Fig. 3.13 for a quartz sphere approaching a quartz surface, thereby enhancing the potential for removal. Other studies also show that surfactants have a significant impact on particle−surface interaction forces [89,100−102].

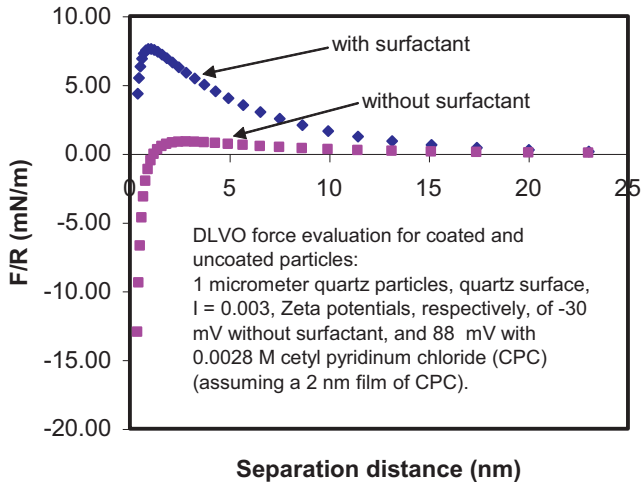

FIGURE 3.13 Comparison of normalized DLVO force (normalized by dividing by particle radius) versus separation distance for quartz particles approaching a quartz surface. Note that the Hamaker constant was calculated using Eq. (3.14) with refractive index and dielectric constant data from Ref. [64]. The forces were calculated using Eqs. (3.9−3.11), (3.13), and (3.14). Note that the zeta potential values shown in the figure are values that were measured using ground quartz and alumina particles in a 0.003 M KCl solution at 22°C. The surface potential was calculated based upon the zeta potentials using the relationship: ψ = zeta potential [exp(−χ/1 nm)] (assumes that the zeta potential is 1 nm from surface).

3.6 Measurement of Particle Removal

Particle removal effectiveness is nearly always measured by optical methods. One simple approach is to capture digital images of appropriately magnified sections of a surface that has residual particles. The digital images can then be analyzed using image analysis software to determine the number of residual particles. A similar method that is often used in the microelectronics industry to inspect wafer contamination involves the use of laser scanning and associated detectors that measure light that is scattered by particles or defects on the surface.

3.7 Enhanced Particle Removal Results Associated With Surfactant Use

Surface force calculations show that surface forces can be reduced significantly by the presence of surfactant, and it is, therefore, anticipated that the addition of sufficient surfactant will enhance particle removal. Several studies show that surfactants can assist in reducing the number of residual particles on a surface [103–107]. Several sets of particle removal data are presented in Figs. 3.14–3.21. Each figure shows that the presence of surfactant has a significant influence on the removal of particles from the associated substrates. Figs. 3.14–3.16 and 3.18–3.21 show that the effectiveness of particle removal generally increases with increasing surfactant concentration. The observed removal effect associated with increasing surfactant

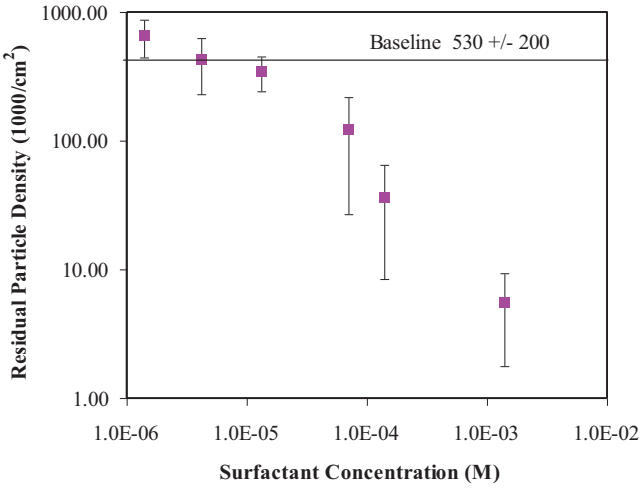

FIGURE 3.14 Residual particle density following chemical mechanical polishing (CMP) processing on copper in 1% ferric nitrate medium versus cetylpyridinium chloride concentration at 31°C.

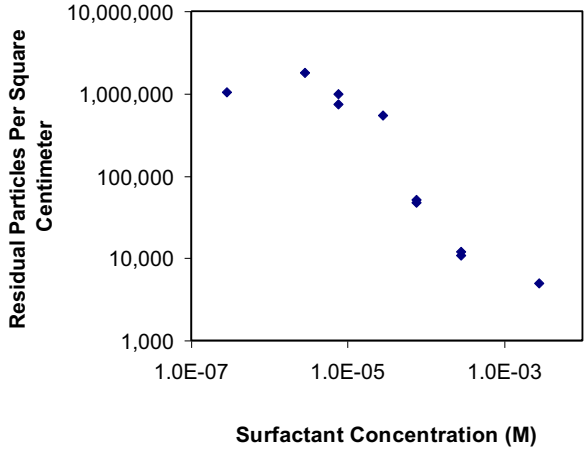

FIGURE 3.15 Comparison of residual particle density and CPC concentration following polishing of a tungsten-coated surface using 0.7-μm-diameter alumina particles.

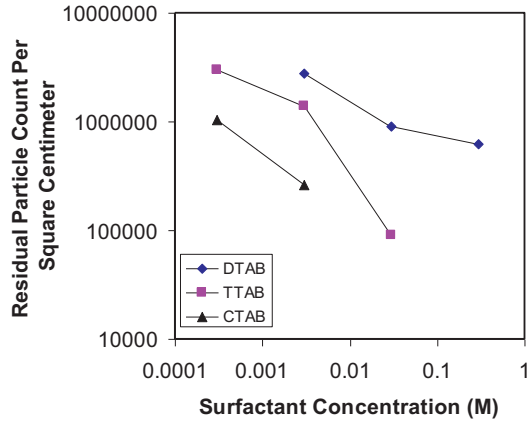

FIGURE 3.16 Comparison of residual particle density and surfactant concentration following polishing of a tungsten-coated surface using 0.7-μm-diameter alumina particles. *CTAB*, Cetyl trimethyl ammonium bromide; *DTAB*, dodecyl trimethyl ammonium bromide; *TTAB*, tetradecyl trimethyl ammonium bromide.

concentration in Fig. 3.19 is generally consistent with the theoretical force considerations that were presented in Figs. 3.12 and 3.13, which predicted an attractive force without surfactant and a repulsive force with sufficient surfactant.

Fig. 3.19 shows that the effectiveness of the surfactant is significantly greater above the cmc. Because the cmc is generally significantly greater than the sac due to higher interfacial free energy at solid surfaces relative to the air–water interface, it is likely that the removal is largely ineffective

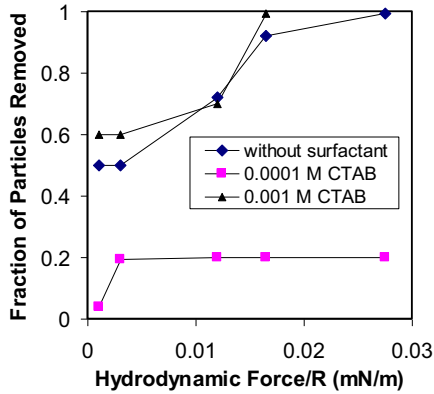

FIGURE 3.17 Effect of cetyl trimethyl ammonium bromide concentration on the removal of 10-μm hydrophilic glass particles from a hydrophilic oxidized silicon wafer substrate. The *x*-axis shows the hydrodynamic removal force due to fluid flow that is normalized by dividing by the particle radius to give a quantitative assessment of the relative removal force. *CTAB*, Cetyl trimethyl ammonium bromide. *Data adapted from Ref. [78].*

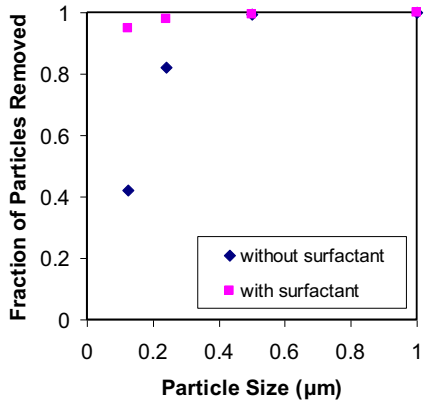

FIGURE 3.18 Polystyrene latex particle removal efficiency versus particle size from silicon substrates using 0.5% hydrofluoric acid (HF) with and without 1% anionic surfactant. *Adapted from Ref. [107].*

below the sac. However, Fig. 3.17 shows that if the adsorption of surfactant onto a hydrophilic substrate leads to a hydrophobic surface as depicted in Fig. 3.10 through the adsorption of less than a bilayer or multilayer, removal is inhibited (see the data for 1×10^{-4} M surfactant, which is below the sac). However, above the sac, the surface becomes hydrophilic as depicted in Fig. 3.10 and removal is facilitated (see the 1×10^{-3} M data set in Fig. 3.17). These findings suggest that for hydrophilic substrate/particle

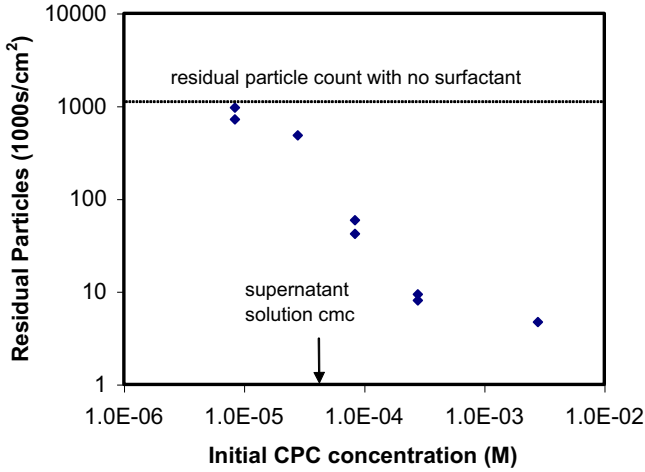

FIGURE 3.19 Comparison of residual particle density and cetylpyridinium chloride (CPC) concentration following the polishing of quartz glass using 0.7-μm-diameter alumina particles. Note that the cmc of the supernatant solution, which is based upon the total CPC added to solution, is much higher than the normal cmc (3×10^{-4} M) due to surfactant adsorption on alumina particles. In other words the supernatant cmc indicates that the free, nonadsorbed surfactant concentration is close to the normal cmc even though the initial CPC concentration was much higher.

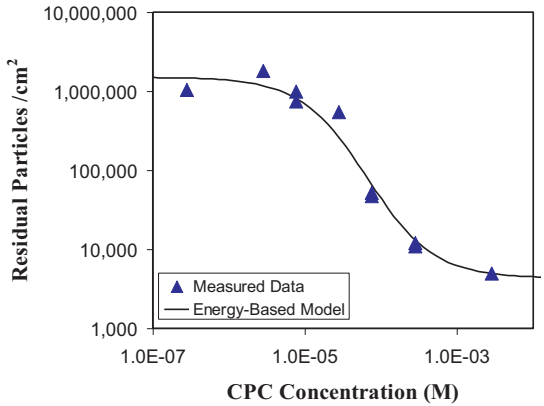

FIGURE 3.20 Comparison of residual particle density and CPC concentration following the polishing of quartz glass using 0.7-μm-diameter alumina particles in 1% ferric nitrate medium at 31°C. The energy-based model fit, which is shown as the solid line, used the following parameters: $P_0 = 1\ 500\ 000$ particles per cm^2, $z = 14\ 500$, K/sac = 15 000 L/mol, and $n = 0.99$.

systems, the equilibrium solution surfactant concentration should exceed the sac for maximum cleaning benefits.

In contrast, however, the results shown in Fig. 3.17 also lead to the inference that if the surfaces are naturally hydrophobic, enhanced removal will

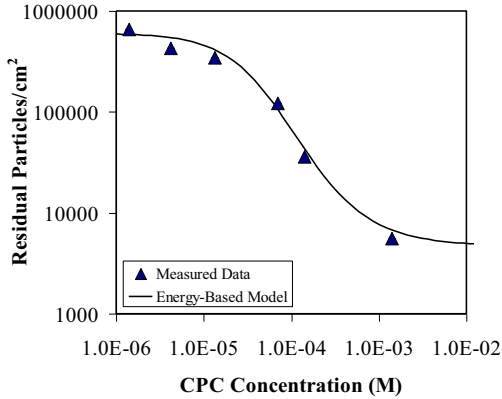

FIGURE 3.21 Comparison of residual particle density and CPC concentration following polishing using 0.7-μm-diameter alumina particles on copper in 1% ferric nitrate medium at 31°C. The energy-based model fit, which is shown as the solid line, used the following parameters: $P_0 = 600\,000$ particles per cm^2, $z = 12\,000$, K/sac = 11 500 L/mol, and $n = 1.27$.

likely be achieved with surfactant at concentrations below the sac. This inference can be explained on the basis of surface hydrophilicity. Because the surface will become more hydrophilic and charged with increasing surfactant adsorption below the sac, the potential for hydrophobic attraction will be minimized and the opportunity for particle removal will be enhanced. It will also be enhanced above the sac, since additional adsorption above the monolayer level occurs in paired layers or micelles, which always have exposed hydrophilic interfaces. Therefore, to maintain efficient particle removal, the bulk concentration of surfactant usually should be well above the sac and the cmc (usually a few times greater than the sac or the cmc) as adsorption at the surface, and precipitation or complexation with contaminants, depletes the free surfactant molecule concentration to well below the level added initially.

However, it should be understood that hydrophobicity/hydrophilicity cleaning prediction discounts the effect of surface charging that is associated with surfactant adsorption as discussed in connection with electrostatic forces. Consequently, it is possible to observe enhanced particle removal when the surfaces have less than bilayer or multilayer coverage of surfactant molecules. However, due to the competing electrostatic repulsion and hydrophobic attraction associated with surfactant coverage below the multilayer level, particle removal is not likely to be as effective as it would be with coverage above the multilayer level, which occurs above the sac.

Nonionic surfactant molecules have been tested for their ability to assist in particle removal, but they tend not to perform as well as ionic surfactants [103]. This finding is not surprising when it is considered that the effect of enhanced favorable electrostatic forces can be generated by the adsorption of ionic surfactant but not of nonionic surfactant.

The overall surfactant cleaning results show that the effect of surfactant adsorption on surface charge, surface hydrophobicity/hydrophilicity, and steric interactions is significant within the context of enhancing particle removal. The results also highlight the importance of understanding the natural surface charge and hydrophobicity/hydrophilicity as well as the sac, which are strong functions of ionic strength and surfactant properties as discussed previously in Section 2. In comparing cleaning data sets, it is also important to account for the difference between equilibrium and initial surfactant concentrations, which are often very different due to the high surface area associated with fine particles that can adsorb large quantities of surfactant and reduce the surfactant concentration in solution.

3.8 Postcleaning Surfactant Removal

After removing particles with the assistance of a surfactant, it is often necessary to remove the residual surfactant. Because most surfactant adsorption events are physical in nature, the surfactant can be removed, to some extent, by simply rinsing the surface. However, because adsorbed surfactant molecules bond with each other, they can resist removal during rinsing with pure water. Their resistance to removal is related to the number of carbons in the hydrocarbon chain. The longer the hydrocarbon segment, the more resistant it is to removal. The resistance to removal can be overcome to some extent through the addition of effective ions that compete for surface adsorption sites, form complexes, or react with the adsorbed surfactant. It has been shown that the exposure of CPC-coated tungsten surfaces to a solution of 1 M ammonium hydroxide for 5 minutes results in the removal of the CPC, whereas simple rinsing in deionized water is only partially successful in removing the surfactant molecules [108]. The rare exception to easy removal with appropriate ions is the removal of chemisorbed surfactant molecules, which may require more aggressive removal environments.

3.9 Selection of Surfactants for Cleaning Purposes

The selection of surfactant molecules for enhanced particle removal from surfaces should involve the assessment of several important factors. One important selection criterion is the charge states of the surfactant and the surfaces to be cleaned. Particle removal works best with charged surfactants, and most surfactants used in any cleaning system are mixtures of ionic and nonionic surfactants except in the cases where highly porous foam filter is required for the cleaning process. Because of the negatively charged nature of most surfaces, anionic surfactants tend to be more efficient for particle removal than cationic surfactants (cationic surfactants themselves are also difficult to remove from these surfaces). Nonionic surfactants are usually more effective in particle removal than cationic surfactants but not as

efficient as anionic surfactants. For ionic surfactants the same charge can build up on the particle and on the solid surface, aiding in particle removal via charge repulsion. Excluded volume interactions between nonionic surfactants and surfaces can be achieved due to the steric effect, although these are not as effective as electrostatic interaction induced by surfactant charging.

Another selection criterion is the behavior of the surfactant molecule at the temperature of the application. Some surfactants have low solubility at the temperature of the desired application and should not be considered. Most often solubility is controlled predominantly by the number of hydrocarbon units in the alkyl chain, so chain length is an important parameter to consider with respect to solubility issues. Although increasing the chain length reduces solubility, it increases surfactant adsorption and aggregation tendencies. Consequently, the effect of chain length must be balanced between adsorption and solubility considerations.

Other factors that need to be considered are functional groups and the application environment. Anionic surfactants are not effective in highly acidic media because they form precipitates, and cationic surfactants are not effective in highly alkaline media due to precipitation. Zwitterionic surfactants are usually only effective in solutions with a near-neutral pH and the absence of highly charged ions. Some environments that contain highly charged ions may induce the precipitation of surfactant ions with opposite charges. Nonionic surfactant molecules are not subject to the same precipitation concerns, although their solubility can change significantly with temperature.

In addition, price consideration is another selection criterion for surfactant selection for particle removal; typical cationic surfactants are usually approximately three times more expensive than typical anionic surfactants [37], so the ionic surfactant adopted is usually anionic.

3.10 Mathematical Modeling of Enhanced Particle Removal Using Surfactants

Recent modeling efforts have shown that enhanced particle removal using surfactants can be predicted using an adsorption site inhibition or an energy-based approach [109]. The adsorption site inhibition approach consists of traditional Langmuir adsorption modeling with the assumption that surfactant coverage is not limited to surface adsorption sites on the surface of a solid substrate. Instead, it is asserted that adsorption sites are limited by the interaction of surfactant with the substrate and/or a surfactant covered substrate. Consequently, the coverage used in the Langmuir adsorption model for the site inhibition approach is an effective coverage that is limited by a combination of factors such as interfacial charge, surface sites, and surfactant adsorption. Although this modeling approach tends to fit residual particle density

data well for most typical data ranges, it does not predict a lower limit for enhanced particle removal.

The energy-based approach, which utilizes an energy-based equation that has a functional form analogous to the Arrhenius equation, has been shown to be a more effective approach to the modeling of enhanced particle removal using surfactants than the adsorption site inhibition model [109]. The energy-based model leads to the next equation [109]:

$$P = P_0 \exp\left[z\left(\frac{(KC/\text{sac})}{(1+KC/\text{sac})}\right)^n\right] \tag{3.16}$$

where P is the residual particle density with surfactant present, P_0 is the residual particle density without surfactant present, z is an energy-based constant, K is a surfactant adsorption constant, C is the surfactant concentration, sac is the surface aggregation concentration, and n is a constant.

The value of P_0 can be obtained by direct measurement. A plot of ln|ln (P_0/P)| versus the natural logarithm of $(1 + KC/\text{sac})/(KC/\text{sac})$ can be used to calculate the other constants based on the rearranged form of the energy-based residual particle density modeling equation:

$$\ln\left|\ln\left(\frac{P_0}{P}\right)\right| = n\ln(z) + n\ln\left(\frac{(1 + KC/\text{sac})}{(KC/\text{sac})}\right) \tag{3.17}$$

Thus, the slope of the resulting plot will be equal to n and the value of n, combined with the intercept of the plot, can be used to determine z. The value of sac can be estimated using Eq. (3.5). The value of K can be estimated using surface tension plots, corrosion inhibition data, or Langmuir–Blodgett film compression tests [110]. The results of the fit of the energy-based model to residual particle density data, which are presented in Figs. 3.17 and 3.18, show that this modeling approach is effective in predicting the effect of surfactant in enhancing alumina particle removal from both quartz and copper substrates.

4 Summary

Surfactants can enhance particle removal from surfaces by modifying the particle–surface interaction forces. Adsorbed surfactant molecules can alter the van der Waals attractive force, electrostatic force, hydrophobic force, as well as provide a steric barrier to contact. The effect of surfactant on these forces can result in greatly enhanced particle removal efficiency.

Surfactant adsorption density and structure are important factors in determining removal enhancement performance associated with surfactants. Cleaning is generally most effective above the sac, which for naturally hydrophilic surfaces allows for bilayer or multilayer level surfactant coverage that provides significant charge repulsion as well as a steric barrier.

Adsorption below the monolayer level renders naturally hydrophilic substrates hydrophobic, which tends to reduce removal efficiency. In contrast, naturally hydrophobic surfaces are likely to benefit from both submonolayer and multilayer coverages of surfactant that occur, respectively, below and above the sac. Existing adsorption theory and available formulas can aid in the prediction of the sac, which is an important parameter in predicting the performance of surfactants in particle removal enhancement. Equations are also available to predict the effectiveness of surfactants in enhancing particle removal.

Acknowledgment

The work of Y. Zhu was partially performed under the auspices of the US Department of Energy by Lawrence Livermore National Laboratory (LLNL) under Contract DE-AC52-07NA27344.

References

[1] F. Zhang, A. Busnaina and G. Ahmadi, "Particle Adhesion and Removal in Chemical Mechanical Polishing and Post-CMP Cleaning", J. Electrochem. Soc. 146, 2665 (1999).

[2] R. Vos, K. Xu, M. Lux, W. Fyen, R. Singh, Z. F. Chen, P. W. Mertens, Z. Hatcher and M. M. Heyns, "Use of Surfactants for Improved Particle Performance of dHF-Based Cleaning Recipes", Solid State Phenom. 76–77, 263 (2001).

[3] J. S. Jeon and S. Raghavan, Wettability and Cleaning of Silicon Wafers in Tetramethyl Ammonium Hydroxide-Based Solutions, In: *Proceedings of the 39th Annual Technical Meeting IEST*, Institute of Environmental Sciences and Technology (IEST), Mount Prospect, IL (1993), pp. 268–273.

[4] M. A. Fury, "Emerging Developments in CMP for Semiconductor Planarization", Solid State Technol. 38, 47 (1995).

[5] T. L. Meyers, M. A. Fury and W. C. Krusell, "Post-Tungsten CMP Cleaning: Issues and Solution", Solid State Technol. 38, 59 (1995).

[6] M. A. Martinez, "Chemical-Mechanical Polishing: Route to Global Polishing", Solid State Technol. 37, 26 (1994).

[7] W. J. Patrick, W. L. Guthrie, C. L. Standley and P. M. Schiable, "Application of Chemical Mechanical Polishing to the Fabrication of VLSI Circuit Interconnections", J. Electrochem. Soc. 138, 1778 (1991).

[8] A. Iqbal, S. R. Roy, G. B. Shinn, S. Raghavan, R. Shah and S. Peterman, "Investigating the Effect of Secondary Platen Pressure on Post-Chemical Mechanical Planarization Cleaning", Microcontamination 12, 45 (1994).

[9] Y. Hayashi, M. Sakurai, T. Nakajima, K. Hayashi, S. Sakaki, S.-I. Chicaki and T. Kunio, "Ammonium Salt Added Silica Slurry for Chemical Mechanical Polishing of the Interlayer Dielectric Film Planarization in ULSIs", Jpn. J. Appl. Phys. 34, 1037 (1995).

[10] F. B. Kaufman, D. B. Thompson, R. E. Broadie, M. A. Jaso, W. L. Guthrie, D. J. Pearson and M. B. Small, "Chemical Mechanical Polishing for Fabricating Patterned W Metal Features as Chip Interconnects", J. Electrochem. Soc. 138, 3460 (1991).

[11] M. Itano, F. W. Kern Jr., M. Miyashita and T. Ohmi, "Particle Removal from Silicon Wafer Surface in Wet Cleaning Process", IEEE Trans. Semicond. Manuf. 6, 258 (1993).

[12] S. Verhaverbeke, R. Messoussi, H. Morinaga and T. Ohmi, "Recent Advances in Wet Processing Technology and Science", Mater. Res. Soc. Symp. Proc. 386, 3 (1995).
[13] H. Fusstetter, A. Schnegg, D. Graf, H. Kirschner, M. Brohl and P. Wagner, "Impact of Chemomechanical Polishing on the Chemical Composition and Morphology of the Silicon Surface", Mater. Res. Soc. Symp. Proc. 386, 97 (1995).
[14] D. J. Riley and R. G. Carbonell, "Mechanisms of Particle Deposition from Ultra-pure Chemicals onto Semiconductor Wafers: Deposition from Bulk Liquid During Wafer Submersion", J. Colloid Interface Sci. 158, 259 (1993).
[15] S. R. Roy, I. Ali, G. Shinn, N. Furusawa, R. Shah, S. Peterman, K. Witt, S. Eastman and P. Kumar, "Postchemical-Mechanical Planarization Cleanup Process for Interlayer Dielectric Films", J. Electrochem. Soc. 142, 216 (1995).
[16] M. Itano, T. Kezuka, M. Ishii, T. Unemoto and M. Kubo, "Minimization of Particle Contamination During Wet Processing of Si Wafers", J. Electrochem. Soc. 142, 971 (1995).
[17] Y. Ein-Eli, E. Abelev, E. Rabkin and D. Starovetsky, "The Compatibility of Copper CMP Slurries with CMP Requirements", J. Electrochem. Soc. 150, C646 (2003).
[18] T. C. Hu, S. Y. Chiu, B. T. Dai, M. S. Tsai, I.-C. Tung and M. S. Feng, "Nitric Acid-Based Slurry with Citric Acid as an Inhibitor for Copper Chemical Mechanical Polishing", Mater. Chem. Phys. 61, 169 (1999).
[19] K. Reinhardt and W. Kern, (Eds.), , William Andrew Imprint, Elsevier, Oxford, UK (2018).
[20] L. Rocchetti, A. Amato and F. Beolchini, "Printed Circuit Board Recycling: A Patent Review", J. Clean. Prod. 178, 814 (2018).
[21] M. K. Jain, Mechanical Scrubbing for Particle Removal, United States Patent 5,551,986 (1996).
[22] A. Sethuraman and W. C. Koutny, Jr., System for Cleaning a Surface of a Dielectric Material, United States Patent 6,302,766 (2001).
[23] K. Ueki, Semiconductor Wafer Cleaning Method Using a Semiconductor Wafer Cleaning Device that Supports a Lower Surface of the Wafer, United States Patent 6,254,690 (2001).
[24] W. C. Krusell, J. M. de Larious and J. Zhang, "Mechanical Brush Scrubbing for Post-CMP Clean", Solid State Technol. 38, 109 (1995).
[25] M. Alessandri, E. Bellandi, F. Pipia, F. Cazzaniga, K. Wolke and M. Schenkl, "Particle Removal Efficiency and Silicon Roughness in HF-DIW/O_3/Megasonics Cleaning", Solid State Phenom. 65–66, 27 (1999).
[26] Y. Nishiyama, T. Kujime and T. Ohmi, Mechanism of Particle Contamination Removal by Megasonic, In: *Proceedings of the 42nd Annual Technical Meeting IEST*, Institute of Environmental Sciences and Technology, Mount Prospect, IL (1996), pp. 100–105.
[27] T. H. Kuehn, D. B. Kittelson, Y. Wu and R. Gouk, "Particle Removal from Semiconductor Wafers by Megasonic Cleaning", J. Aerosol Sci. 27, S427 (1996).
[28] G. Gale, A. Busnaina, F. Dai and I. Kashkoush, "How to Accomplish Effective Megasonic Particle Removal", Semicond. Intl. 19, 4 (1996).
[29] J. M. Lee, K. G. Watkins and W. M. Steen, "Angular Laser Cleaning for Effective Removal of Particles from a Solid Surface", Appl. Phys. A 71, 671 (2000).
[30] A. Rosenfeld, D. Ashkenasi, H. Varel, M. Waehmer and E. E. B. Campbell, "Time Resolved Detection of Particle Removal from Dielectrics on Femtosecond Laser Ablation", Appl. Surf. Sci. 127, 76 (1997).
[31] R. Kohli, "Applications of Water Ice Blasting for Removal of Surface Contaminants", in: *Developments in Surface Contamination and Cleaning: Applications of Cleaning Techniques*, Volume 11, R. Kohli and K. L. Mittal (Eds.), Elsevier, Oxford, UK (2019).

[32] R. Sherman, "Carbon Dioxide Snow Cleaning", in: *Developments in Surface Contamination and Cleaning: Fundamentals and Applied Aspects*, Volume 1, 2nd Edition, R. Kohli and K. L. Mittal (Eds.), Elsevier, Oxford, UK (2016).
[33] S. Jantzen, T. Decarreaux, M. Stein, K. Kniel and A. Dietzel, "CO_2 Snow Cleaning of Miniaturized Parts", Precision Engineering 52, 122 (2018).
[34] S. Banerjee, "Cryoaerosol Cleaning of Particles from Surfaces", in: *Particle Adhesion and Removal*, K. L. Mittal and R. Jaiswal (Eds.), Wiley-Scrivener, Beverly, MA (2015), pp. 453–476.
[35] K. Gotoh, "Cleaning Applications Using a High-Speed Impinging Air Jet", in: *Developments in Surface Contamination and Cleaning: Applications of Cleaning Techniques*, Volume 11, R. Kohli and K. L. Mittal (Eds.), Elsevier, Oxford, UK (2019).
[36] M. L. Free, "The Use of Surfactants to Enhance Particle Removal from Surfaces", in: *Developments in Surface Contamination and Cleaning: Fundamentals and Applied Aspects*, Volume 1, 2nd Edition, R. Kohli and K. L. Mittal (Eds.), Elsevier, Oxford, UK (2016).
[37] B. Grady, "The Use of Surfactants to Enhance Particle Removal from Surfaces", in: *Particle Adhesion and Removal*, K. L. Mittal and R. Jaiswal (Eds.), Wiley-Scrivener, Beverly, MA (2015), pp. 453–476.
[38] J. N. Israelachvili, *Intermolecular and Surface Forces*, 3rd Edition, Academic Press Imprint, Elsevier, Oxford, UK (2011).
[39] P. C. Hiemenz and R. Rajagopalan, *Principles of Colloid and Surface Science*, 3rd Edition, Marcel Dekker, New York, NY (1997).
[40] M. L. Free, W. Wang and D. Y. Ryu, "Prediction of Corrosion Inhibition Using Surfactants", Corrosion 60, 837 (2004).
[41] Y. Zhu, M. L. Free and G. Yi, "Electrochemical Measurement, Modeling, and Prediction of Corrosion Inhibition Efficiency of Ternary Mixtures of Homologous Surfactants in Salt Solution", Corros. Sci. 98, 417 (2015).
[42] Y. Zhu, M. L. Free and G. Yi, "The Effects of Surfactant Concentration, Adsorption, Aggregation, and Solution Conditions on Steel Corrosion Inhibition and Associated Modeling in Aqueous Media", Corros. Sci. 102, 233 (2016).
[43] Y. Zhu, M. L. Free and J. Cho, "Integrated Evaluation of Mixed Surfactant Distribution in Water-Oil-Steel Pipe Environments and Associated Corrosion Inhibition Efficiency", Corros. Sci. 110, 213 (2016).
[44] M. L. Free, "The Development and Application of Useful Equations to Predict Corrosion Inhibition by Different Surfactants in Various Aqueous Environments", Corrosion 58, 1025 (2002).
[45] J. F. Zemaitis Jr., D. M. Clark, M. Rafal and N. C. Scrivner, *Handbook of Aqueous Electrolyte Thermodynamics*, American Institute of Chemical Engineers, John Wiley and Sons, Hoboken, NJ (1986).
[46] K. S. Pitzer, *Activity Coefficients in Electrolyte Solutions*, 2nd Edition, CRC Press, Taylor & Francis Group, Boca Raton, FL (1991).
[47] Y. Zhu, M. L. Free and G. Yi, "Experimental Investigation and Modeling of the Performance of Pure and Mixed Surfactant Inhibitors: Aggregation, Adsorption, and Corrosion Inhibition on Steel Pipe in Aqueous Phase", J. Electrochem. Soc. 162, C582 (2015).
[48] Y. Zhu and M. L. Free, "Experimental Investigation and Modeling of the Performance of Pure and Mixed Surfactant Inhibitors: Micellization and Corrosion Inhibition", Colloids Surf. A 489, 407 (2016).

[49] J. N. Butler, *Ionic Equilibrium: Solubility and pH Calculations*, John Wiley and Sons, Hoboken, NJ (1998).

[50] R. Nagarajan, "One Hundred Years of Micelles; Evolution of the Theory of Micellization", in: *Surfactant Science and Technology: Retrospects and Prospects (in Honor of Kash Mittal)*, L. S. Romsted (Ed.), CRC Press, Taylor & Francis Group, Boca Raton, FL (2014), pp. 1–110.

[51] V. Srinivasan and D. Blankschtein, "Prediction of Conformational Characteristics and Micellar Solution Properties of Fluorocarbon Surfactants", Langmuir 21, 1647 (2005).

[52] L. Moreira and A. Firoozabadi, "Molecular Thermodynamics for Micellar Branching in Solutions of Ionic Surfactants", Langmuir 26, 15177 (2010).

[53] V. A. Andreev and A. I. Victorov, "Molecular Thermodynamics for Micellar Branching in Solutions of Ionic Surfactants", Langmuir 22, 8298 (2006).

[54] S. V. Koroleva and A. I. Victorov, "Modeling of the Effects of Ion Specificity on the Onset and Growth of Ionic Micelles in a Solution of Simple Salts", Langmuir 30, 3387 (2014).

[55] A. Shiloach and D. Blankschtein, "Predicting Micellar Solution Properties of Binary Surfactant Mixtures", Langmuir 14, 1618 (1998).

[56] A. Shiloach and D. Blankschtein, "Prediction of Critical Micelle Concentration of Nonideal Ternary Surfactant Mixtures", Langmuir 14, 4105 (1998).

[57] S. Manne, J. P. Cleveland, H. E. Gaub, G. D. Stucky and P. K. Hansma, "Direct Visualization of Surfactant Hemimicelles by Force Microscopy of the Electrical Double Layer", Langmuir 10, 4409 (1994).

[58] V. K. Paruchuri, A. V. Nguyen and J. D. Miller, "Zeta-Potentials of Self-Assembled Surface Micelles of Ionic Surfactants Adsorbed at Hydrophobic Graphite Surfaces", Colloids Surf. A 250, 519 (2004).

[59] G. Srinivas, S. O. Nielsen, P. B. Moore and M. L. Klein, "Molecular Dynamics Simulations of Surfactant Self-Organization at a Solid-Liquid Interface", J. Am. Chem. Soc. 128, 848 (2006).

[60] W. Weber, P. H. Hunenberger and J. A. McCammon, "Molecular Dynamics Simulations of a Polyalanine Octapeptide Under Ewald Boundary Conditions: Influence of Artificial Periodicity on Peptide Conformation", J. Phys. Chem. B 104, 3668 (2000).

[61] C. D. Bruce, M. L. Berkowitz, L. Perera and M. D. E. Forbes, "Molecular Dynamics Simulation of Sodium Dodecyl Sulfate Micelle in Water: Micellar Structural Characteristics and Counterion Distribution", J. Phys. Chem. B 106, 3788 (2002).

[62] Y. Tang, L. Yao, C. Kong, W. Yang and Y. Chen, "Molecular Dynamics Simulations of Dodecylamine Adsorption on Iron Surfaces in Aqueous Solution", Corros. Sci. 53, 2046 (2011).

[63] Y. Zhu, M. L. Free, R. Woollam and W. Durnie, "A Review of Surfactants as Corrosion Inhibitors and Associated Modeling", Prog. Mater. Sci. 90, 159 (2017).

[64] R. G. Horn, "Surface Forces and Their Actions in Ceramic Materials", J. Am. Ceram. Soc. 73, 1117 (1990).

[65] M. L. Free and D. O. Shah, "The Role of Cetyl Pyridinium Chloride in Reducing Adhesion Forces Between Alumina Particles and Quartz Surfaces", in: *Particles on Surfaces 5 & 6: Detection, Adhesion, and Removal*, K. L. Mittal (Ed.), VSP, Utrecht, The Netherlands (1999), pp. 95–106.

[66] V. V. Yaminsky, B. W. Ninham, H. K. Christenson and R. M. Pashley, "Adsorption Forces Between Hydrophobic Monolayers", Langmuir 12, 1936 (1996).

[67] W. A. Ducker, Z. Xu, D. R. Clarke and J. N. Israelachvili, "Forces Between Alumina Surfaces in Salt Solutions: Non-DLVO Forces and the Implications for Colloidal Processing", J. Am. Ceram. Soc. 77, 437 (1994).

[68] G. Binnig, C. Gerber, E. Stoll, T. R. Albrecht and C. F. Quate, "Atomic Resolution with Atomic Force Microscope", Europhys. Lett. 3, 1281 (1987).
[69] K. L. Johnson and H. M. Pollock, "The Role of Adhesion in the Impact of Elastic Spheres", J. Adhes. Sci. Technol. 8, 1323 (1994).
[70] D. S. Rimai, D. J. Quesnel and R. Reifenberger, "The Adhesion of Irregularly-Shaped 8 μm Diameter Particles to Substrates: The Contributions of Electrostatic and van der Waals Interactions", J. Adhes. 74, 283 (2000).
[71] J. K. Vrtis, C. D. Athanasiou, R. J. Farris, L. P. DeMejo and D. S. Rimai, "Surface Force Induced Deformations: A Post Particle Removal Examination of the Substrate", J. Adhes. Sci. Technol. 8, 929 (1994).
[72] D. S. Rimai, L. P. DeMejo and R. C. Bowen, "Mechanics of Particle Adhesion", J. Adhes. Sci. Technol. 8, 1333 (1994).
[73] S. K. Das, R. S. Schechter and M. M. Sharma, "The Role of Surface Roughness and Contact Deformation on the Hydrodynamic Detachment of Particles from Surfaces", J. Colloid Interface Sci. 164, 63 (1994).
[74] M. van den Tempel, "Interaction Forces Between Condensed Bodies in Contact", Adv. Colloid Interface Sci. 3, 137 (1972).
[75] K. L. Mittal, (Ed.), , CRC Press, Boca Raton, FL (2000).
[76] E. G. Kelly and D. J. Spottiswood, *Introduction to Mineral Processing*, John Wiley and Sons, Somerset, NJ (1982).
[77] N. de Nevers, *Fluid Mechanics*, Addison-Wesley Publishing Company, Reading, MA (1970).
[78] A. M. Freitas and M. M. Sharma, "Effect of Surface Hydrophobicity on the Hydrodynamic Detachment of Particles from Surfaces", Langmuir 15, 2466 (1999).
[79] M. A. Hubbe, "Theory of Detachment of Colloidal Particles from Flat Surfaces Exposed to Flow", Colloids Surf. 12, 151 (1984).
[80] F. Didier and J. Jupille, "The van der Waals Contribution to the Adhesion Energy at Metal-Oxide Interfaces", Surf. Sci. 314, 378 (1994).
[81] S. Veeramasuneni, M. R. Yalamanchili and J. D. Miller, "Measurement of Interaction Forces Between Silica and α-Alumina by Atomic Force Microscopy", J. Colloid Interface Sci. 184, 594 (1996).
[82] J. J. Adler, Y. I. Rabinovich, R. K. Singh and B. M. Moudgil, "Surface-Particle Interactions in the Chemical Mechanical Polishing Process", Mater. Res. Soc. Symp. Proc. 501, 387 (1998).
[83] S. Veeramasuneni, M. L. Free and J. D. Miller, "Usefulness of Surfactants in Reducing Particle Adhesion and their Effectiveness in Cleaning Silicon Wafers", J. Adhes. Sci. Technol. 12, 185 (1998).
[84] J.-P. Hsu and Y.-C. Kuo, "Electrostatic Interaction Force Between a Charge-Regulated Particle and a Rigid Surface", J. Colloid Interface Sci. 183, 194 (1996).
[85] F. Podczeck, J. M. Newton and M. B. James, "Assessment of Adhesion and Autoadhesion Forces Between Particles and Surfaces. Part II. The Investigation of Adhesion Phenomena of Salmeterol Xinafoate and Lactose Monohydrate Particles in Particle-on-Particle and Particle-on-Surface Contact", J. Adhes. Sci. Technol. 9, 475 (1995).
[86] Y.-L. Ong, A. Razatos, G. Georgiou and M. M. Sharma, "Adhesion Forces Between *E. coli* Bacteria and Biomaterial Surfaces", Langmuir 15, 2719 (1999).
[87] Z. Xu, R. Chi, T. Difeo and J. A. Finch, "Surface Forces Between Sphalerite and Silica Particles in Aqueous Solutions", J. Adhes. Sci. Technol. 14, 1813 (2000).
[88] C. E. McNamee, Y. Tsujii, H. Ohshima and M. Matsumoto, "Interaction Forces Between Two Surfaces in Particle-Containing Aqueous Systems", Langmuir 20, 1953 (2004).

[89] B. V. Derjaguin, I. N. Aleinikova and Y. P. Toporov, "Role of Electrostatic Forces in the Adhesion of Polymer Particles to Solid Surfaces", Prog. Surf. Sci. 45, 119 (1994).
[90] E. L. Nagaev, "Surface Forces and Chemical Potential of Small Particles", Phys. Status Solidi B 167, 381 (1991).
[91] A. Busnaina, J. Taylor and I. Kashkoush, "Measurement of the Adhesion and Removal Forces of Submicrometer Particles on Silicon Substrates", J. Adhes. Sci. Technol. 7, 441 (1993).
[92] Z. Xu, W. Ducker and J. N. Israelachvili, "Forces Between Crystalline Alumina (Sapphire) Surfaces in Aqueous Sodium Dodecyl Sulfate Surfactant Solutions", Langmuir 12, 2263 (1996).
[93] L. P. Xu, S. Pradhan and S. Chen, "Adhesion Forces Studies of Janus Nanoparticles", Langmuir 23, 8544 (2007).
[94] T. M. Pan, T. F. Lei, F. H. Ko, T. S. Chao, M. C. Liaw, Y. H. Lee and C. P. Lu, "Performance Evaluation of Cleaning Solutions Enhanced with Tetraalkylammonium Hydroxide Substituents for Post-CMP Cleaning on Poly-Si Film", J. Electrochem. Soc. 149, G336 (2002).
[95] T. H. Tsai and Y. F. Wu, "Effects of Nonionic Surfactants on Performance of Copper Chemical Mechanical Polishing", Chem. Eng. Commun. 193, 702 (2006).
[96] D. Ng, P. Y. Huang, Y. R. Jeng and H. Liang, "Nanoparticle Removal Mechanisms During Post-CMP Cleaning", Electrochem. Solid State Lett. 10, H227 (2007).
[97] S. Mingbin, G. Baohong, W. Chenwei, M. Yingxin, D. Bo and T. Baimei, "Nonionic Surfactant on Particles Removal in Post-CMP Cleaning", J. Semiconductors 36, 026002 (2015).
[98] S. Banerjee, S. Sutanto, J. M. Kleijn and M. A. C. Stuart, "Towards Detergency in Liquid CO_2 – A Surfactant Formulation for Particle Release in an Apolar Medium", Colloid Surf. A 415, 1 (2012).
[99] Y. Wang, "The Model of Nano-Scale Cu-Particle Removal in CO_2-Based Micelle Solutions with Different Surfactants", Adv. Mater. Res. 936, 624 (2014).
[100] A. Zelenev, V. Privman and E. Matijevic, "Effects of Surfactants on Particle Adhesion. II. Interactions of Monodispersed Colloidal Hematite with Glass Beads in the Presence of 1-Dodecylpyridinium Chloride", Colloids Surf. A 135, 1 (1998).
[101] M. Nose, M. Itano and T. Ohmi, "Particle Deposition Control for Various Wafer Surfaces in Acidic Solution with Surfactant", Part. Sci. Technol. 14, 27 (1996).
[102] K. Wong, K. Ramkumar, H. Bamnolker, S. Puri, R. Bhushan, D. Wong, G. Elmore and R. Mohindra, Ultra-Low Particle Semiconductor Cleaner for Removal of Particle Contamination and Residues from Surface Oxide Formation on Semiconductor Wafers, United States Patent 6,004,399 (1999).
[103] M. L. Free and D. O. Shah, "Using Surfactants in Iron-Based CMP Slurries to Minimize Residual Particles", Micro 16, 29 (1998).
[104] M. Bielmann, U. Mahajan, R. K. Singh, D. O. Shah and B. J. Palla, "Enhanced Tungsten Chemical Mechanical Polishing Using Stable Alumina Slurries", Electrochem. Solid State Lett. 2, 148 (1999).
[105] M. L. Free and D. O. Shah, "Enhancement of Particle Removal and Modification of Interfacial Phenomena Using Surfactants", in: *Particles on Surfaces 7: Detection, Adhesion, and Removal*, K. L. Mittal (Ed.), VSP, Utrecht, The Netherlands (2002), pp. 405–418.
[106] M. L. Free, "The Use of Surfactants to Reduce Particulate Contamination on Surfaces", in: *Particles on Surfaces 8: Detection, Adhesion, and Removal*, K. L. Mittal (Ed.), VSP, Utrecht, The Netherlands (2003), pp. 129–139.

[107] R. Vos, K. Xu, G. Vereecke, F. Holsteyns, W. Fyen, L. Wang, J. Lauerhaas, M. Hoffman, T. Hackett, P. W. Mertens and M. M. Heyns, "Advanced Wet Cleaning of Sub-micrometer Sized Particles", in: *Particles on Surfaces 8: Detection, Adhesion, and Removal*, K. L. Mittal (Ed.), VSP, Utrecht, The Netherlands (2003), pp. 255–270.

[108] M. L. Free and D. O. Shah, "Adsorption and Desorption of Cetyl Pyridinium Ions at a Tungsten-Coated Silicon Wafer Surface", J. Colloid Interface Sci. 208, 104 (1998).

[109] M. L. Free, "Prediction of Particle Removal Using Surfactants", in: *Particles on Surfaces 9: Detection, Adhesion, and Removal*, K. L. Mittal (Ed.), CRC Press, Taylor & Francis Group, Boca Raton, FL (2006), pp. 317–328.

[110] M. L. Free, "A New Corrosion Inhibition Model for Surfactants that more Closely Accounts for Actual Adsorption than Traditional Models that Assume Physical Coverage is Proportional to Inhibition", Corros. Sci. 46, 3101 (2004).

This page intentionally left blank